ground water

Case Study/

Groundwater Recharge at Five Representative Sites in the Hebei Plain, China

by Xiaohui Lu[1,3], Menggui Jin[1], Martinus Th. van Genuchten[2], and Bingguo Wang[1]

Abstract

Accurate estimates of groundwater recharge are essential for effective management of groundwater, especially when supplies are limited such as in many arid and semiarid areas. In the Hebei Plain, China, water shortage is increasingly restricting socioeconomic development, especially for agriculture, which heavily relies on groundwater. Human activities have greatly changed groundwater recharge there during the past several decades. To obtain better estimates of recharge in the plain, five representative sites were selected to investigate the effects of irrigation and water table depth on groundwater recharge. At each site, a one-dimensional unsaturated flow model (Hydrus-1D) was calibrated using field data of climate, soil moisture, and groundwater levels. A sensitivity analysis of evapotranspirative fluxes and various soil hydraulic parameters confirmed that fine-textured surface soils generally generate less recharge. Model calculations showed that recharge on average is about 175 mm/year in the piedmont plain to the west, and 133 mm/year in both the central alluvial and lacustrine plains and the coastal plain to the east. Temporal and spatial variations in the recharge processes were significant in response to rainfall and irrigation. Peak time-lags between infiltration (rainfall plus irrigation) and recharge were 18 to 35 days in the piedmont plain and 3 to 5 days in the central alluvial and lacustrine plains, but only 1 or 2 days in the coastal plain. This implies that different time-lags corresponding to different water table depths must be considered when estimating or modeling groundwater recharge.

Introduction

The Hebei plain is one of the most productive agricultural areas of northern China, occupying an area of about 73,000 km^2 and having a population of approximately 50 million. Groundwater is the main source of water, with agricultural usage about 70% of total water use. Excessive use of both surface and groundwater in this densely populated semiarid plain has led to a rapid decline of groundwater levels since the 1980s, as well as aggravated environmental problems. The fresh water table is declining at a rate of 1 to 2 m/year, with the total decline during the past decades being 10 to 30 m in many areas. Especially affected is the piedmont plain to the west where the water table is currently at depths of up to 60 m or more. Furthermore, water levels in fresh confined aquifers have declined to 100 m below surface in many parts of the plain, even in areas where levels were originally near (or even above) land surface. Water shortage and associated environmental problems are increasingly threatening the local socio-economic sustainability of the area (Jin et al. 1999; Yang et al. 2006).

The long-term natural groundwater cycle in the Hebei plain has been greatly changed over the years due to human activities. Vertical groundwater recharge from

[1]Corresponding author: MOE Key Laboratory of BGEG, Institute of Water Resources and School of Environmental Studies, China University of Geosciences, Wuhan, Hubei 430074, China; 86-27-67883461; fax: 86-27-87436235; mgjin@cug.edu.cn

[2]Department of Mechanical Engineering, LTTC/COPPE, Federal University of Rio de Janeiro, UFRJ, Rio de Janeiro, RJ 21945-970, Brazil.

[3]School of Earth Sciences and Engineering, Hohai University, Nanjing, Jiangshu, 210098, China.

Received January 2009, accepted December 2009.

doi: 10.1111/j.1745-6584.2009.00667.x

precipitation and irrigation return flow, and evapotranspiration (ET) are the main components of the water cycle in the plain, with the unsaturated zone playing an important role. Water-saving agricultural practices since the 1990s, along with the declining water tables and increased thickness of the vadose zone, have strongly affected the recharge processes and net groundwater recharge (Jin et al. 2000; Wang et al. 2008a). As in many other arid and semiarid areas of the world with limited groundwater resources, knowledge of how the groundwater recharge alters with changes in natural and anthropogenic factors is critical for effective management of available water supplies.

Groundwater recharge in the Hebei plain is generally estimated using empirical equations, usually by simply multiplying the precipitation rate by an empirical recharge coefficient; these values are used in groundwater flow models (Wang et al. 2008b). This empirical approach does not consider explicitly the effects of local land use, irrigation, and water table depth on recharge.

The main objective of this study is to provide a more process-based investigation of the effects of irrigation and water table depth on groundwater recharge in the Hebei plain. The Hydrus-1D variably saturated flow model (Šimůnek et al. 2005) was used at five representative sites. Hydrus-1D has been widely used to simulate a broad range of water flow and solute transport processes in variably saturated media (Šimůnek et al. 2008, and references therein), although applications to recharge processes have been relatively limited (Scanlon et al. 2003; Jimenez-Martinez et al. 2009). Additional objectives were used to evaluate temporal and spatial variability in the recharge processes in the Hebei plain. The study also provided an opportunity for comparing recharge rates estimated with unsaturated flow modeling to those derived using chemical tracer studies (e.g., Wang et al. 2008a) at similar sites.

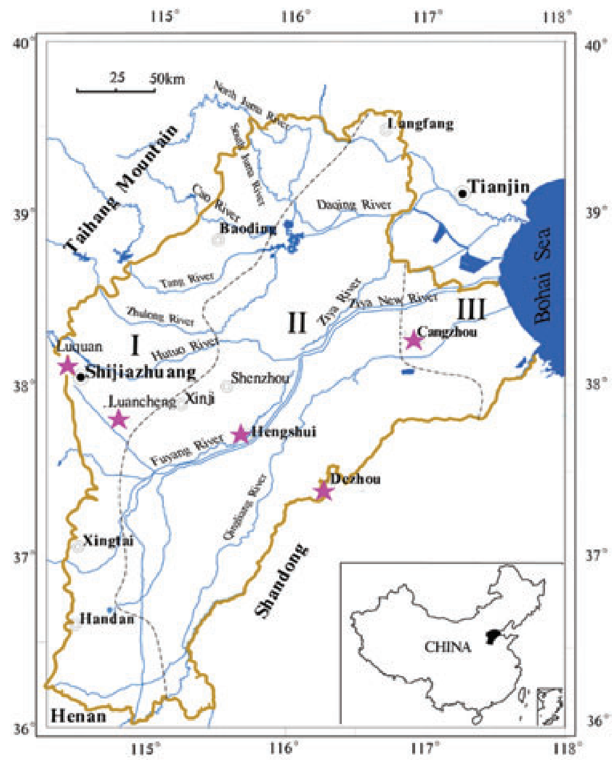

Figure 1. Locations of the five representative sites in the Hebei plain, showing the location of the five sites (stars), rivers (in blue), boundaries of the study area (in brown), and boundaries of geomorphological units (dashed line). The roman numerals indicate: the piedmont plain (I), the alluvial and lacustrine plains (II), and the coastal plain (III).

Site and Data Description

The Hebei plain is a semiarid to semi-humid area with a monsoon-dominated climate. Mean annual precipitation is 500 to 600 mm, of which more than 80% occurs in the months of June through September, whereas mean annual evaporation rates (of open water) are in the order of 1000 to 1300 mm (Chen et al. 2008). Geomorphologically, the Hebei plain comprises three parts from west to east: the piedmont plain, the alluvial and lacustrine plains, and the coastal plain (Figure 1). The water table in the piedmont plain is relatively deep, generally 10 to 40 m, but up to 60 m at some locations, whereas the unsaturated zone consists mainly of silt and fine sand (Table 1). The water table depth in the alluvial and lacustrine plains is in the order of 1 to 20 m, with the unsaturated zone mostly consisting of silty clay and silt. By comparison, the water table is relatively shallow in the coastal zone near the Bohai Sea, generally between 1 and 4 m below the land surface.

Five representative sites in the Hebei plain were selected for the recharge studies (Table 1): the Luquan (LQ) and Luancheng (LC) sites in the piedmont plain to the west, the Hengshui (HS) and Dezhou (DZ) sites

Table 1
General Features of the Representative Sites

Site	Geomorphology	Water Table Depth (m)	Lithology
Qijie in LQ	Piedmont plain	10–25	Silt and fine sand
LC	Piedmont plain	30–35	Silty clay
HS	Alluvial and lacustrine plains	3–5	Silty clay, clay, and silt
DZ	Alluvial and lacustrine plains	2–6	Silty clay
CZ	Coastal plain	1–4	Silt and silty clay

in the central alluvial and lacustrine plains, and the Cangzhou (CZ) site in the coastal plain to the east (Table 1 and Figure 1). Soil water contents, pressure heads, and groundwater levels were monitored every 5 to 10 days from 2003 to 2005. Pressure heads were measured using tensiometers. Water contents were measured using an L520 neutron probe (Jiangsu Academy of Agricultural Sciences, Nanjing, China) at the LC and HS sites, and using MP160 moisture probes (ICT International Pty Ltd., Armidale, Australia) at the other sites. Daily meteorological data were obtained from local weather stations, which were all located on site, except for the LQ weather station, which was located about 5 km from the LQ study site. Water used for irrigation was estimated by agricultural researchers or local farmers (based on electricity use).

Mathematical Model

The Hydrus-1D software package (Šimůnek et al. 2005) was used to simulate 1D vertical flow assuming applicability of the standard Richards equation for unsaturated flow as follows:

$$\frac{\partial \theta(h)}{\partial t} = \frac{\partial}{\partial z}\left[K(h)\left(\frac{\partial h}{\partial z}+1\right)\right] - S(h) \qquad (1)$$

subjected to the initial and boundary conditions

$$h(z,0) = h_0(z) \qquad (2)$$

$$-K(h)\left(\frac{\partial h}{\partial z}+1\right)\bigg|_{z=0} = q_0(t) \qquad (3)$$

$$\frac{\partial h}{\partial z}(L,t) = 0 \qquad (4a)$$

or

$$h(L,t) = h_L(t) \qquad (4b)$$

where θ is the volumetric water content [—], h is the pressure head [L], z is the vertical coordinate [L], assumed to be 0 at the soil surface and directed upward, t is time [T], K is the unsaturated hydraulic conductivity [L T^{-1}], S is a sink term to account for root water uptake [T^{-1}], $h_0(z)$ is the initial condition, and $q_0(t)$ is the fluid flux across the soil surface boundary [L T^{-1}]. As the lower boundary condition (Equations 4a,b), we implemented either a free drainage condition, $\partial h/\partial z = 0$, when the water table was relatively deep (the LQ and LC sites), or a time variably pressure head condition, $h_L(t)$, when the water table was relatively close to the soil surface (the HS, DZ, and CZ sites).

Following Feddes et al. (1978), root water uptake was modeled using the function

$$S(h) = \lambda(z)\alpha(h)T_{\mathrm{p}} \qquad (5)$$

where $\lambda(z)$ is the relative root distribution function [—], T_{p} is the potential transpiration rate [L T^{-1}], and $\alpha(h)$ is a dimensionless water stress response function ($0 \le \alpha \le 1$) to account for reductions in uptake due to drought stress [—].

For $\alpha(h)$, we adopted the functional form of Feddes et al. (1978) using Hydrus-1D default parameter values for wheat and maize based on studies by Taylor and Ashcroft (1972) and Wesseling (1991). This function assumes that within some pressure head range $h_3 \le h \le h_2$ root water uptake is optimal. Below h_3, root water uptake declines from 1.0 to 0 at h_4 (the wilting point) due to water stress. Above h_2, root water uptake similarly declines linearly from 1.0 to 0 at h_1 due to insufficient aeration. The critical pressure head h_3 increases for higher potential transpiration rates, T_{p}. The Hydrus-1D default parameters of wheat used in this study were: $h_1 = 0$ cm, $h_2 = -1$ cm, $h_{3\mathrm{l}} = -500$ cm, $h_{3\mathrm{h}} = -900$ cm, $h_4 = -16{,}000$ cm. The default parameters of maize were: $h_1 = -15$ cm, $h_2 = -30$ cm, $h_{3\mathrm{l}} = -325$ cm, $h_{3\mathrm{h}} = -600$ cm, $h_4 = -8000$ cm (Wesseling 1991).

For $\lambda(z)$, we used a linear root distribution varying between 0 at the bottom of the root zone and 1.0 at the soil surface (Feddes et al. 2001; Mertens et al. 2006). Observed plant root data in the Hebei plain indicated that, on average, the rooting depth of winter wheat increased from approximately 15 cm in March to 75 cm in May, and the rooting depth of summer maize from 0 cm on June 6 to 15 cm on July 2, and to 40 cm on August 1, and to a final 45 cm on September 1.

The surface boundary Equation 3 was implemented as an atmospheric condition without surface ponding in which $q_0(t)$ equals precipitation plus irrigation minus potential evaporation as long as the pressure head determined at the soil surface exceeds some minimum negative value ($-10{,}000$ cm in our study). However, the boundary flux becomes a time-variable flux during periods of high evaporation as determined by the pressure head distribution near the soil surface with $h(0,t) = -10{,}000$ cm. Surface runoff was assumed to occur when the surface becomes saturated, in which $q_0(t)$ in Equation 3 decreases in value. Equation 3 was implemented using daily precipitation, irrigation, and ET rates.

Simulations based on Equation 1 were applied to the five sites using a self-adjusting numerical time stepping scheme, and with finite element discretizations in which nodal spacings generally ranged from 1 cm near the soil surface up to a maximum of 10 cm at the bottom of the flow domain for deep water tables (the DZ site). The simulation period for model calibration was from January 1, 2003 to August 31, 2005, whereas groundwater recharge rates at the sites were calculated from January 1, 2004 to December 31, 2004, using initial conditions of January 1, 2003. Annual (2004) rainfall and irrigation rates at the sites are given in Table 2.

Unsaturated Soil Hydraulic Properties

The solution of Equations 1 through 4 requires estimates of the soil water retention, $\theta(h)$, and unsaturated hydraulic conductivity, $K(h)$, relationships. We used the

Table 2
Rainfall and Irrigation in 2004 at the Five Sites

Items	LQ	LC	HS	DZ	CZ
Rainfall (mm)	434.6	456.7	434.6	534.5	447.8
Irrigation (mm)	375	300	225	300	225

van Genuchten (1980) soil hydraulic functions

$$\theta(h) = \begin{cases} \theta_r + \dfrac{\theta - \theta_s}{[1+|\alpha h|^n]^m} & h < 0 \ (m = 1 - 1/n) \\ \theta_s & h \geq 0 \end{cases} \quad (6)$$

$$K(h) = \begin{cases} K_s S_e^{1/2}[1-(1-S_e^{1/m})^m]^2 & h < 0 \\ K_s & h \geq 0 \end{cases} \quad (7)$$

where θ_r and θ_s are the residual and saturated water contents [—], respectively, α [L^{-1}] and n [—] are empirical shape factors that depend on soil type, K_s is the saturated hydraulic conductivity [L T^{-1}], and S_e is effective saturation given by

$$S_e(h) = \frac{\theta(h) - \theta_r}{\theta_s - \theta_r} \quad (8)$$

Soil water retention data were measured in the laboratory on undisturbed soil cores taken from the field sites (Lu et al. 2006). Measurements were made for pressure heads between 0 and about −800 cm, whereas water contents (including θ_s) were measured gravimetrically. The parameters θ_r, α, and n were subsequently fitted to the observed retention data using the RETC program of van Genuchten et al. (1991).

Measurements of the vertical saturated hydraulic conductivity, K_s, were obtained in the laboratory using falling head experiments on undisturbed soil cores taken from several depths at the LC and HS sites. For the LC site, we obtained K_s values of 42.0, 28.6, and 41.4 cm/d for the 0 to 20, 35 to 50, and 280 to 310 cm soil layers, respectively. For the HS site, measured K_s values were 143.6, 35.3, and 84.8 cm/d, respectively, for cores taken from depths of 0 to 30, 50 to 70, and 200 to 220 cm, respectively. Saturated hydraulic conductivities of the other sites were estimated from measured particle distributions and soil textural averages using the Rosetta pedotransfer functions of Schaap et al. (1998) as implemented in Hydrus-1D. All the laboratory-measured hydraulic parameters were considered to be initial estimates subjected to further calibration against observed soil water content time series measured at the field sites.

Evapotranspiration

In this study, we used the Penman-Monteith equation (Allen et al. 1998; Liu et al. 1997) to estimate the reference crop evapotranspiration rate, ET_0 (mm/d), as follows:

$$ET_0 = \frac{0.408\Delta(R_n - G) + \dfrac{900}{T+273}\gamma u_2(e_a - e_d)}{\Delta + \gamma(1 + 0.34u_2)} \quad (9)$$

where R_n is net solar radiation (J/m^2/d), G is soil heat flux (J/m^2/d), e_a is the saturation water vapor pressure at mean air temperature (kPa), e_d is the mean actual vapor pressure (kPa), Δ is the slope of the saturation vapor pressure (kPa/°C), γ is the psychrometric constant (kPa/°C), and u_2 is wind speed at a height of 2 m (m/s). Potential ET_p (mm/d) was calculated using the formula:

$$ET_p = K_c \cdot ET_0 \quad (10)$$

where K_c is a dimensionless crop coefficient. As crop coefficients for both the HS and DZ sites of the alluvial and lacustrine plains we used values estimated by Chen and Guo (1993) at a geomorphologically similar site near Gaocheng in Hebei Province. The crop coefficients for the experimental sites at LC and LQ were based on data obtained by Zhang (2002) for a site near LC in the piedmont plain (Table S1, Supporting Information).

The potential evaporation rate of a soil under a standing crop was derived from the Penman-Monteith equation by neglecting the aerodynamic term. The only source of energy for soil evaporation is then net radiation that reaches the soil surface (Ritchie 1972). Assuming that net radiation inside a canopy decreases according to an exponential function, and that the soil heat flux can be neglected, we can derive (Goudriaan 1977; Belmans et al. 1983):

$$E = E_p e^{-K_{gr}\mathrm{LAI}} \quad (11)$$

where E is the soil evaporation [—], K_{gr} is the extinction coefficient for solar radiation [—], and LAI is the Area Index of wheat or maize [—]. Ritchie (1972) and Feddes (1978) both used $K_{gr} = 0.39$.

Daily potential transpiration rates (T_p) were calculated by subtracting evaporation from total ET. Estimated potential evaporation and transpiration rates at the five sites are shown in Figure S1, Supporting Information.

Results and Discussion

Simulations of the Field Soil Moisture Dynamics

Initial simulations using the laboratory estimated unsaturated soil hydraulic parameters, or those estimated using pedotransfer functions, were found to be relatively poor and in need of improvement. For these reasons, we used the Hydrus-1D inverse module (Šimůnek et al. 2005) at all the sites to improve estimates of the hydraulic parameters in terms of providing optimal descriptions of the field data. Because of the large number of parameters involved for the layered profiles, many of them correlated, values of selected parameters (notably the parameter n) were adjusted only when the

Table 3
Calibrated Soil Hydraulic Parameters of the Five Sites

Representative Sites	Depth (cm)	Materials	θ_r	θ_s	α	n	K_s (cm/d)
LQ	0–500	Silt	0.068	0.400	0.0010	2.400	69.0
LC	0–42.5	Silty clay	0.086	0.360	0.0134	1.574	33.5
	42.5–90	Silty clay	0.089	0.361	0.0315	1.179	28.7
	90–3300	Silty clay and silt	0.099	0.365	0.0151	1.747	23.3
HS	0–50	Silt	0.068	0.400	0.0020	2.320	93.3
	50–150	Clay	0.110	0.410	0.0110	1.480	30.5
	150–400	Silty clay	0.080	0.390	0.0070	2.060	82.0
DZ	0–140	Silt	0.090	0.360	0.0060	1.660	50.0
	140–510	Silt	0.068	0.400	0.0010	2.400	69.0
CZ	0–300	Silty clay	0.086	0.360	0.0134	1.574	33.5

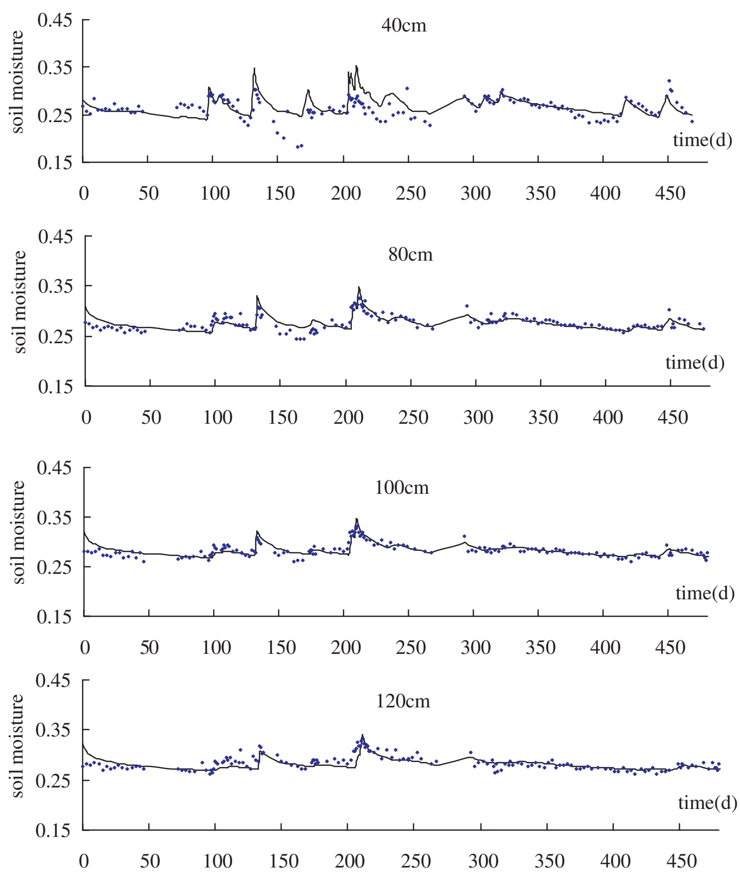

Figure 2. Comparison between measured (dots) and simulated (lines) volumetric water contents of different depths at the Luancheng site.

differences between the calculated and field-measured water contents were larger than the standard deviation. The final identified parameters for the five sites (Table 3) provided a close fit between simulated and measured water contents, as illustrated for the LC site in Figure 2 using data from four depths.

Temporal and Spatial Changes in Recharge

Temporal variations in the vertical groundwater recharge rate depend mainly on the temporal distributions of water input (precipitation and irrigation) and ET. Figure 3 shows the calculated daily recharge rate as well as rainfall plus irrigation at the LC site from January 1, 2003 to August 31, 2005. The recharge rate from January to March was less than 1 mm/d due to low rainfall and the absence of any irrigation. Recharge then gradually increased from April to September because of irrigation in April and May, and because of more rainfall from June to September. Starting at the end of September, the recharge rate decreased again. Figure 3 also indicates that

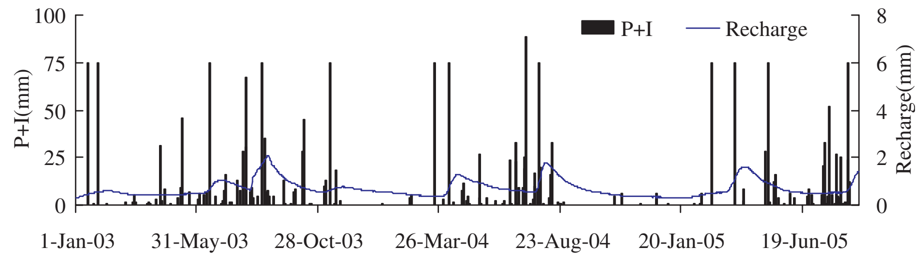

Figure 3. Daily recharge and rainfall plus irrigation rates for the Luancheng site (from January 1, 2003 to August 31, 2005).

Table 4
Summary of 2004 Simulation Results Obtained for the Five Study Sites

Geomorphology	Water Table Depth (m)	Site	R (mm)	R_r (mm/d)	R_c (%)
Piedmont plain	10-40	LQ	169	0.46	21
		LC	180	0.49	24
Alluvial and lacustrine plains	2–20	HS	140	0.38	21
		DZ	155	0.43	19
Coastal plain	<5	CZ	102	0.28	15

Note: R is the total 2004 recharge, R_r is the average daily groundwater recharge rate, R_c is the recharge coefficient (%).

the recharge peaks are delayed relative to the maxima in precipitation and irrigation. Antecedent moisture conditions and the time period over which rainfall occurs appear equally or more important than the total quantity of rainfall. For example, the intense rain storms generated more recharge during the summer monsoon season than did the totality of smaller precipitation events and irrigation applications during the remainder of the year.

Figure S2 (Supporting Information) shows daily recharge rates vs. precipitation plus irrigation ($P + I$) at all the five sites for 2004. The LQ and LC sites in the piedmont plain, both having deep water tables (Table 1), showed the longest time-lags between the rainfall and irrigation events and recharge. The HS and DZ sites in the alluvial and lacustrine plains, where water tables were intermediate in depth, showed much shorter time-lags between the rainfall and irrigation events and recharge. Recharge at the CZ site in the coastal plain showed no obvious time-lag after a rainfall or an irrigation event. Recharge of groundwater in the more humid piedmont plain was always larger than that in the alluvial and lacustrine plains and the coastal plain.

The simulation results for 2004 are further summarized in Table 4. They show that both the average recharge rate R_r and the recharge coefficient R_c reduce gradually from the piedmont plain to the coastal plain.

Relation Between Precipitation and Recharge in the Hebei Plain

The results in Figures 3 and S2 (Supporting Information) indicate that the total amount of recharge through the unsaturated zone is mostly determined by the totality of the local precipitation, irrigation, and ET rates, whereas water table depth and the lithology of the unsaturated zone (and hence soil moisture storage in the unsaturated zone) determine the time delays and the degree of smoothing in the recharge rates relative to the precipitation and irrigation events. For example, the water table in CZ is relatively shallow, which causes the infiltrated water to reach the water table relatively quickly so that most of the individual rainfall/irrigation corresponds to isolated infiltration recharge events with very small time-lags (generally only about 1 or 2 days).

Following Wu et al. (1996), we used the peak time-lag here as the time elapsed from the beginning of an individual rainfall event to the time at which the recharge rate reaches its maximum, and the cessation time-lag as the time elapsed from the beginning of rainfall to the cessation of recharge. As the depth to water table increased, the correspondence between rainfall and recharge decreased. The water table depths at the DZ and HS sites were in the order of 2 to 5 m, which caused the recharge events produced by several individual rainfalls to merge into one single process, although a few smaller recharge peaks still corresponded to some of the larger rainfall events or concentrated rainfall clusters. A peak in the annual recharge process represents an integrated recharge event produced by a set of individual rains clustered around a large rainfall event corresponding to this peak. The peak time-lags at DZ and HS were generally between about 3 and 5 days.

By comparison, the water tables at the LQ and LC sites are relatively deep, thus requiring much more time for the infiltrated water to reach the water table. The peak time-lags at these sites were between 18 and 35 days or more. The peak at LQ in late March was different from those at the other sites due to early irrigation and having higher initial soil water contents. Recharge after the peak

Table 5
Comparisons of Calculated 2004 Recharge Rates Obtained with and Without Accounting for Irrigation

Study Sites	A (Rainfall + Irrigation) R_r (mm/year)	B (Rainfall) R_r (mm/year)	$C = A - B$ (Irrigation Only) R_r (mm/year)	C/A (%)
LQ	169	86	83	49
LC	180	103	77	43
HS	140	83	57	41
DZ	155	126	29	20
CZ	102	75	27	28

decreased smoothly, which is typical for locations with a deep water table.

Analysis of Groundwater Recharge from Irrigation Return Flow

To estimate groundwater recharge from irrigation return flow, we reran the previously calibrated models for the five sites assuming the same climate conditions, but now without irrigation. We assumed that the recharge simulated with both irrigation and rainfall minus the recharge simulated with rainfall only is the recharge stemming from irrigation return flow. The simulation results (Table 5) show that groundwater recharge decreased significantly and that recharge caused by irrigation in the Hebei plain accounted for 27% to 49% of the total precipitation and irrigation. Irrigation-induced recharge at LQ was largest among the five sites (49% of the total precipitation and irrigation). Recharge caused by irrigation in the piedmont plain was slightly larger than that in the alluvial and lacustrine plains.

Comparison of Numerical Results with Chemical Tracer Studies

Wang et al. (2008a) previously used vadose zone chemical (tritium and bromide) tracing to estimate groundwater recharge at similar locations in the Hebei plain as a function of soil type, land use, and irrigation. Figure 4 compares their results for the recharge coefficient R_c, with our numerical simulations for different areas in the Hebei plain. The two approaches give approximately the same results for flood-irrigated croplands, with the locations in the piedmont plain (LC and DZ) showing the highest recharge coefficients. The nonirrigated uncultivated areas showed much lower R_c values, not only in the coastal plain to the east (CZ), but also DZ in the central alluvial and lacustrine plains. It is to be noted that the tracer method gave somewhat higher estimates for the recharge coefficient as compared to the numerical modeling approach.

As compared to the tracer method, numerical simulation is a far more convenient and cost-effective approach, but it requires relatively long-term weather data, information about the local irrigation practices, and soil physical parameters. However, if the data are available, numerical simulation may well be a very attractive alternative to chemical tracer methods.

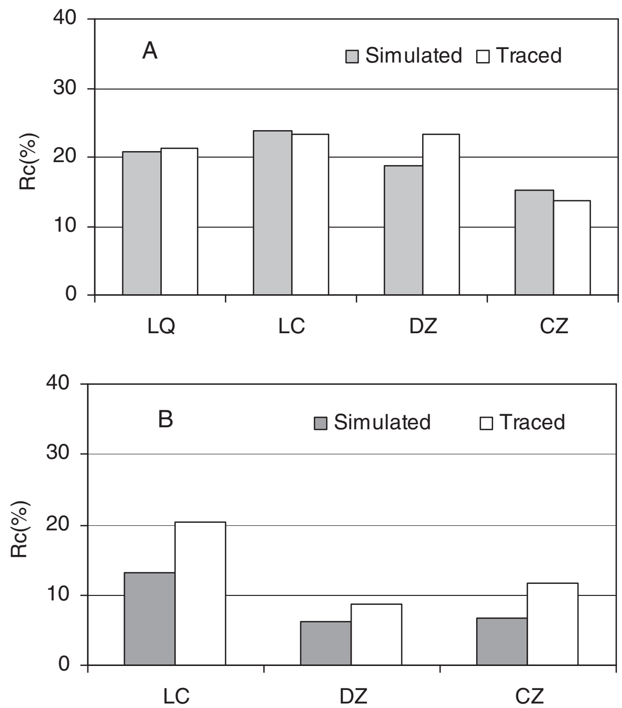

Figure 4. Comparison of the recharge coefficient (R_c) at different locations in the Hebei plain obtained with numerical unsaturated flow modeling (this study) and chemical tracing: (A) flood-irrigated cropland and (B) nonirrigated uncultivated land.

Uncertainty and Sensitivity Assessment

The vadose zone modeling approach used in this study contains several potential sources of uncertainty. Uncertainty exists about the computed infiltration fluxes, ET fluxes, and recharge fluxes. Possible sources of uncertainty are the values of the many model parameters needed to run Hydrus-1D, including the soil hydraulic parameters, parameters in the reference ET rate equation, crop coefficients, and drought stress parameters in the uptake model of Feddes et al. (1978). For the soil hydraulic parameters, information is available in the form of 95% confidence intervals (CI) and correlation coefficients computed using the inverse solution module of Hydrus-1D. Unfortunately, no such information is available about uncertainty in the other model parameters.

Hence, as previously indicated by Jimenez-Martinez et al. (2009) it does not seem possible at this time to place reliable quantitative CI on the computed recharge rates due to a lack of knowledge about parameter variability and correlation structure. Still, some notion of the importance of parameter uncertainty may be obtained by carrying out a sensitivity analysis of various model parameters. Here, we limit the analysis to the soil hydraulic parameters in Equations 6 and 7. Our calculations showed that the order of sensitivity of the parameters for groundwater recharge were: n, θ_s, K_s, α, and θ_r. The residual water content, θ_r, was found to be the least sensitive, consistent with findings by Jimenez-Martinez et al. (2009). Taking the LC site as an example, allowing individual parameters for all layers to decrease or increase by 50% from the calibrated values in Table 3 caused groundwater recharge to change by -18% and $+15\%$ for K_s, -8% and $+6\%$ for α, and $+2\%$ for θ_r, respectively. When decreasing the value of n by 10% or increasing by 10% and 50%, groundwater recharge changed to -24%, $+26\%$, and $+59\%$, respectively. Except those for n, these changes are relatively small and somewhat expected for simulations in which rainfall, irrigation and evaporation rates are mostly imposed as boundary conditions (flux-controlled infiltration), with still important but lesser effects due to water stress. The combined effects of these parameters reflect the fact that fine-textured soils (i.e., those having lower n, K_s, and α values) retain more moisture near the soil surface for subsequent root water uptake and ET, thus generally leading to lower recharge rates (e.g., Kenneth-Smith et al. 1994; Nolan et al. 2003; Jimenez-Martinez et al. 2009).

The sensitivity of ET was calculated by perturbing an input variable by a fixed percentage at all the times during the calibration period. ET in this case was individually increased or decreased by 10%. The model was subsequently run using the perturbed input to obtain the resulting groundwater recharge values. Results show that decreasing or increasing the value of ET by 10% caused the groundwater recharge to change by $+5\%$ and -4%, respectively.

We note that accurate characterization of the prediction uncertainty is problematic because of a lack of knowledge about parameter variability and parameter correlation structure. Future study aimed at quantifying uncertainty in parameters would greatly benefit from more comprehensive analyses of uncertainty in groundwater recharge calculations of the type provided in this study.

Conclusions

Hydrus-1D was found to be a very useful tool for simulating groundwater recharge in the Hebei plain characterized by relatively little topographic relief, relatively deep water tables, and insignificant snowmelt, and with available data limited to the lithology of the unsaturated zone and laboratory-measured soil physical parameters. Our study of recharge at the five representative zones permits several conclusions.

1. Temporal variations in the groundwater recharge rate at the five sites were found to be significant. Groundwater recharge was significantly delayed relative to rainfall or irrigation in the piedmont plain (the LQ and LC sites) and the alluvial and lacustrine plains (DZ and HS), but not obviously so in the coastal plain (CZ). The highest recharge rates to groundwater at the DZ, HS, and LC sites occurred in August, whereas at LQ the highest recharge rates occurred in late March and at CZ in July.

2. The recharge rate was on average 175 mm/year in the piedmont plain, and 133 mm/year in both the alluvial and lacustrine plains and the coastal plain. The average infiltration recharge coefficient in the piedmont plain (0.22) was higher than those of the alluvial and lacustrine plains and the coastal plain (0.18 in both the plains).

3. The peak time-lag between an infiltration event (rainfall or irrigation) in the coastal plain with its shallow water tables was generally at most 1 or 2 days. Peak time-lags for sites in the central alluvial and lacustrine plains were usually about 3 to 5 days, with the recharge peaks often generated by a series of individual rainfalls clustered around some large rainfall event. By comparison, the peak time-lags in the piedmont zone with its much deeper water tables (generally >10 m) were about 18 to 35 days. Recharge rates in this zone were much more gradual with time because of buffering by the deep unsaturated zone. This implies that different time-lags corresponding to different water table depths may need to be considered when estimating or modeling groundwater recharge.

4. Groundwater recharge from irrigation in the Hebei plain accounted for about 27% to 49% of the total precipitation plus irrigation. Of the five sites, LQ showed the highest rate stemming from irrigation (49% of the total precipitation plus irrigation).

5. As compared with the tracer methods, numerical simulation seems a much more convenient and cost-effective approach for estimating groundwater recharge. A disadvantage of unsaturated flow modeling is the need for long-term data about climate, irrigation practices, and soil physical parameters. Still, the numerical approach may be preferred if the required data are available.

Acknowledgments

This study was financed in part by the 863 Program of China (2007AA06Z337), the 973 Program of China (2010CB428802), the China Geology Survey (200310400035-1), the National Natural Science Foundation of China (40772155, 40472123), and CAPES, Brazil. We would also like to thank all the members of the project group for their fruitful collaboration and the China Scholarship Council. We gratefully acknowledge the reviewers (Dr. Phillip Stauffer and two anonymous reviewers) for their constructive comments and suggestions on the article.

Supporting Information

Additional Supporting Information may be found in the online version of this article:

Table S1. Monthly crop coefficients for the Luancheng and Gaocheng experimental sites

Figure S1. Daily potential evaporation and transpiration rates of the five sites

Figure S2. Daily recharge and precipitation plus irrigation ($P + I$) rates in 2004 at the five sites

Please note: Wiley-Blackwell are not responsible for the content or functionality of any supporting materials supplied by the authors. Any queries (other than missing material) should be directed to the corresponding author for the article.

References

Allen, R.G., L.S. Pereira, D. Raes, and M. Smith. 1998. Crop evapotranspiration. Guidelines for computing crop water requirements. Irrigation and Drainage Paper No. 56. FAO, Rome.

Belmans, C., J. Wesseling, and R.A. Feddes. 1983. Simulation function of the water balance of a soil: SWATRE. *Journal of Hydrology* 63, 271–286.

Chen, M., Q. Yin, and T.Y. Zhao. 2008. Evaluation of evaporation in the Hai river basin (in Chinese). *Design of Water Resources and Hydraulic Engineering* 27, no. 2: 11–12.

Chen, Y.M., and G.S. Guo. 1993. *Study on Water Requirement Isoline of the Main Crop of China*. Beijing, China: Agricultural Scientech Press (In Chinese).

Feddes, R.A., H. Hoff, M. Bruen, T. Dawson, P. de Rosnay, R. Dirmeyer, R.B. Jackson, P. Kabat, A. Kleidon, A. Lilly, and A.J. Pitman. 2001. Modeling root water uptake in hydrological and climate models. *Bulletin of the American Meteorological Society* 82, no. 12: 2797–2809.

Feddes, R.A., P.J. Kowalik, and H. Zarandny. 1978. *Simulation of Field Water Use and Crop Yield*. New York: John Wiley Sons.

Goudriaan, J. 1977. Crop meteorology: a simulation study. Simulation monographs, Pudoc, Wageningen.

Jimenez-Martinez, J., T.H. Skaggs, M.Th. van Genuchten, and L. Candela. 2009. A root zone modeling approach to estimating groundwater recharge from irrigated areas. *Journal of Hydrology* 367, no. 1–2: 138–149.

Jin, M.G., R.Q. Zhang, L.F. Sun, and Y.F. Gao. 1999. Temporal and spatial soil water management: a case study in the Heilonggang region, PR China. *Agricultural Water Management* 42, no. 2: 174–187.

Jin, M.G., X. Liang, I. Simmers, Y.F. Gao, and R.Q. Zhang. 2000. Estimation of groundwater recharge using artificial tritium tracing. *Proceedings of the International Symposium on Hydrogeology and the Environment, Wuhan, China*, 17–21 October 2000. China: Environmental Science Press, 340–345.

Kenneth-Smith, A., P.G. Cook, and G.R. Walker. 1994. Factor affecting groundwater recharge following clearing in the south western Murray Bason. *Journal of Hydrology* 154, no. 1: 85–105.

Liu, Y., L.S. Pereira, and J.L. Teieirab. 1997. Update definition and computation of reference evapotranspiration comparison with former method (In Chinese). *Journal Hydraulic Engineering* 6, 27–33.

Lu, X.H., M.G. Jin, and B.G. Wang. 2006. Discussion on the soil water characteristic curve of the agricultural ecosystem experiment station in Luancheng. Hebei China (In Chinese). *Rural Water and Hydropower* 12, 30–32.

Mertens, J., R. Stenger, and G.F. Barkle. 2006. Multiobjective inverse modeling for soil parameter estimation and model verification. *Vadose Zone Journal* 5, no. 3: 917–933.

Nolan, B.T., A.L. Baehr, and L.J. Kauffman. 2003. Spatial variability of groundwater recharge and its effect on shallow groundwater quality in southern New Jersey. *Vadose Zone Journal* 2, 677–691.

Ritchie, J.T. 1972. A model for predicting evaporation from a row crop with incomplete cover. *Water Resource Research* 8, no. 5: 1204–1213.

Scanlon, B., K. Keese, R.C. Reedy, J. Šimůnek, and B. Andraski. 2003. Variations in flow and transport in thick desert vadose zones in response to paleoclimatic forcing (0–90 kyr): monitoring, modeling, and uncertainties. *Water Resource Research* 39, no. 7: 1179. DOI: 10.1029/2002WR001604.

Schaap, M.G., F.J. Leij, and M.Th. van Genuchten. 1998. Neural network analysis for hierarchical prediction of soil hydraulic properties. *Soil Science Society of America Journal* 62, 847–855.

Šimůnek, J., M.Th. van Genuchten, and M. Šejna. 2008. Development and applications of the HYDRUS and STANMOD software packages and related codes. *Vadose Zone Journal* 7, 587–600.

Šimůnek, J., M.Th. van Genuchten, and M. Šejna. 2005. The HYDRUS-1D software package for simulating the one-dimensional movement of water, heat, and multiple solutes in variably-saturated media, Version 3.0, HYDRUS Software Series 1, Department of Environmental Sciences, University of California, Riverside, CA, 270p.

Taylor, S.A., and G.M. Ashcroft. 1972. *Physical Edaphology*, 434–435. San Francisco, California: Freeman and Co.

van Genuchten, M.Th. 1980. A closed-form equation for predicting the hydraulic conductivity of unsaturated soils. *Soil Science Society of America Journal* 44, 892–898.

van Genuchten, M.Th., F.J. Leij, and S.R. Yates. 1991. The RETC code for quantifying the hydraulic functions of unsaturated soils. Report No. EPA/600/2-91/065. Ada, OK: R.S. Kerr Environmental Research Laboratory, U.S. Environmental Protection Agency, 85p.

Wang, B., M. Jin, J.R. Nimmo, L. Yang, and W. Wang. 2008a. Estimating groundwater recharge in Hebei plain, China under varying land use practices using tritium and bromide tracers. *Journal of Hydrology* 356, no. 1–2: 209–222.

Wang, S.Q., J.L. Shao, X.F. Song, Y.B. Zhang, Z.B. Huo, and X.Y. Zhou. 2008b. Application of MODFLOW and geographic information system to groundwater flow simulation in North China Plain, China. *Environmental Geology* 55, no. 7: 1449–1462.

Wesseling, J.G. 1991. Meerjarige simulates van groundwateronttrekking voor verschillende bodemprofielen, grondwatertrappen en gewassen met het model SWATRE. Report 152. Winand Starring Centre, Wageningen.

Wu, J., R. Zhang, and J. Yang. 1996. Analysis of rainfall-recharge relationships. *Journal of Hydrology* 177, no. 1–2: 143–160.

Yang, Y., M. Watanabe, X. Zhang, X. Hao, and J. Zhang. 2006. Estimation of groundwater use by crop production simulated by DSSAT-wheat and DSSAT-maize models in the piedmont. *Hydrological Processes* 20, 2787–2802.

Zhang, X. 2002. Index system for irrigation scheduling of winter wheat and maize in the Piedmont of mountain Taihang (In Chinese). *Transactions of the Chinese Society of Agricultural Engineering* 6, 35–39.